Self-assembly and self-organization : an overview
Application to magnetic materials

Olivier Fruchart

3rd ASI, Sendai (July 2004)

Olivier Fruchart
Laboratoire Louis Néel (CNRS)
25, Avenue des Martyrs – BP166
F-38042 Grenoble Cedex 9
Olivier.Fruchart@grenoble.cnrs.fr
http://lab-neel.grenoble.cnrs.fr/pageperso/fruche/

1 Introduction

A short overview of the field of condensed matter self-organization[1] on surfaces is proposed. The different mechanisms responsible for self-organization will be covered, with examples taken from semiconductors, oxides and metals. Finally, as a specialist of magnetism I will discuss where self-organization can be useful for magnetism.

This document is intended to be an introduction to the field, it remains very general. Readers interested in details should use the references provided.

2 Self-assembled epitaxial growth

2.1 Growth modes in epitaxy

An parameter intuitively acknowledged to influence the way thins films grow is one known from the macroscopic scale: surface[2] and interface energies. In 1958 Bauer formulated a criterium to predict the growth mode of a material f upon deposition on a surface S, called the substrate [10]. Bauer's criterium is based on the evaluation of the quantity $\Delta\gamma = \gamma_S - \gamma_f - \gamma_{\text{int}}$ where γ_S, γ_f and γ_{int} are the energy per unit area of the substrate, of the deposited material, and of their interface, respectively. Wetting should occur for $\Delta\gamma > 0$, *i.e.* for materials of low surface energy deposited on substrates of high surface energy[3]. This mode, called Franck van den Merwe growth mode (FvdM [11]), favors the formation of a continuous film. In the reverse case for $\Delta\gamma < 0$ the formation of *dots* (also called *islands* or *clusters*) on an otherwise bare surface is favored. This latter situation is called the Volmer-Weber growth mode (VW [12]). Another parameter, arising only at the microscopic scale, is the lattice mismatch between substrate and deposit. To adapt the two lattices dislocations tend to form, generally close to the interface, whose cost in elastic energy can be viewed as an additional positive contribution to interfacial energy. This again favors the formation of dots. When wetting should otherwise be expected this leads to a third growth mode, consisting of the wetting of a few atomic layers explained by surface/interface energy arguments, followed by the formation of dots due to lattice mismatch and dislocations formation. This is the Stranski-Krastanov growth mode (SK [13]). Notice that this thermodynamic picture may be hindered by kinetic aspects. A review of growth modes can be found in many references, *e.g.* Ref.4,14,15.

[1] In this document I will call self-assembly (SA) the process by which nanostructures are fabricated spontaneously by deposition on a surface. These nanostructures might be dots, stripes, wires, tubes etc., and in general they display no long-range positional order. I will call self-organization (SO) a special case of SA, that where the nanostructures display a long-range position order. We will see that in most cases the order is caused by self-organization of the substrate surface itself before deposition, not to phenomena related to growth. Note that this definition of SA and SO is not universally admitted in the literature.

[2] see Ref.9 for a review of surface energy of metals

[3] Notice that interface energies are generally not known. Metal-metal interface energies are generally thought to be small compared to surface energies

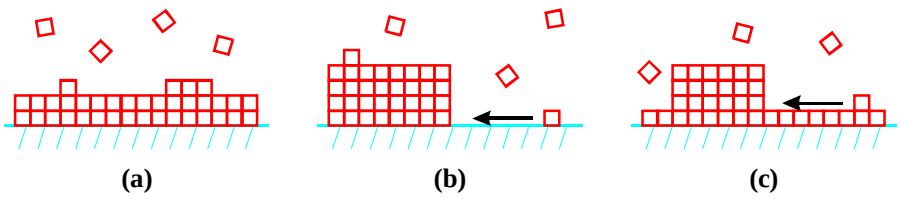

Figure 1: Schematic illustration of the three main growth modes. (a) Frank van den Merwe (b) Volmer-Weber (c) Stranski-Krastanov

SA often rely on SK and VW growth modes, whereas examples of SO are found for all growth modes, as will be seen in the following.

2.2 Macroscopic regime – The shape of compact self-assembled dots

At the macroscopic scale and down to some hundreds of nanometers, the lattice symmetry and lattice parameters of supported dots is usually relaxed to their bulk values [16]. In this case their shape is only determined by the minimization of *surface* plus *interface* energies. It can be predicted straightforwardly using a geometrical construction named Wulff-Kaichev's theorem, based on an extension of the century-old Wulff's theorem for free dots (Ref.17 and included references, and Figure 2). It predicts the distance h_i of each facet i to the (possibly virtual) center of the crystal :

$$\frac{\gamma_i}{h_i} = \frac{(\gamma_{\rm int} - \gamma_{\rm S})}{h_{\rm int}} = \text{constant} \tag{1}$$

where γ_i is the free energy of facet i, $\gamma_{\rm S}$ that of the substrate, and $\gamma_{\rm int}$ is the free interfacial energy between the deposited material and the substrate. For smaller dots' size strain comes into play, and one should use either a modified Wulff-Kaichev's continuum approach [17] or an atomistic calculation.

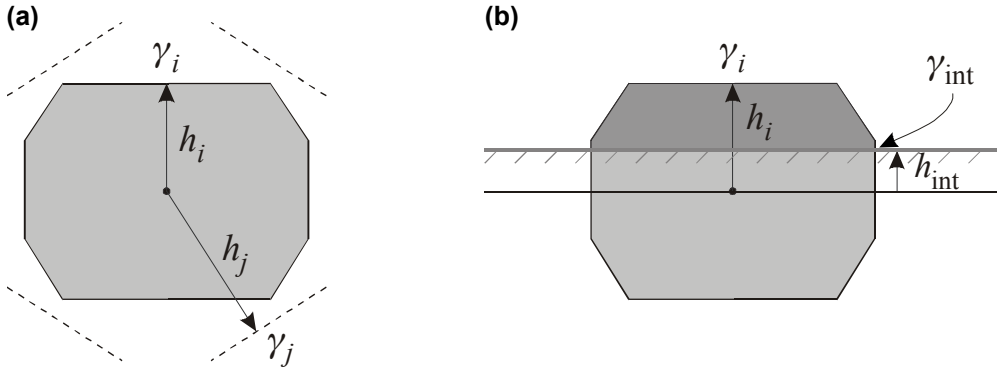

Figure 2: The (a) Wulff [resp. (b) Wulff-Kaischev] theorem predicts the shape of a free-standing (resp. supported) dot as a function of its surface (resp. plus interface) energies.

2.3 The sub-atomic-layer range of deposition

A completely different situation where self-assembly often occurs is when the amount of material deposited is less than one atomic layer. Thus, whether thermodynamics would favor self-assembly or not for thicker deposits, at this early stage there is not enough material to form a continuous film. Thus, the deposit consists of non-percolated patches of material. In the case of VW compact dots occur. In the case of SK or FvdM the islands are very flat, usually one-atomic-layer high. Self-organization is most often obtained in this regime (see next section). Notice finally that a strong miscibility of the deposited material with respect to the substrate might prevent self-assembly.

2.4 Parameters to play with

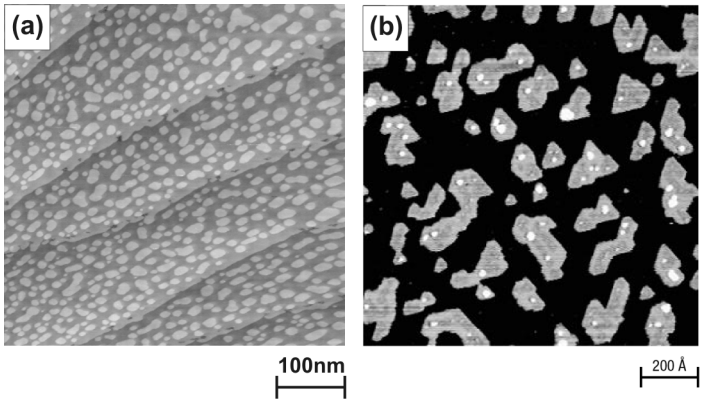

Figure 3: Self-assembly naturally occurs for sub-atomic-layer deposition (a) Fe/Mo(110) [18] (b) Co/Pt(111) [19].

The parameters accessible to the experimentalist to tailor the morphology of SA nanostructures are :

- *Temperature*, that influences the areal density of nanostructures on a defect-free surface. This parameter may not be effective in the case of SO deposition on a pre-patterned surface, see later.
- *Amount of deposited material*. Generally, the higher the deposition temperature, the larger the nanostructures.
- *Symmetry* of both substrate and deposited material, influencing the dot's or wire's shape and facetting.

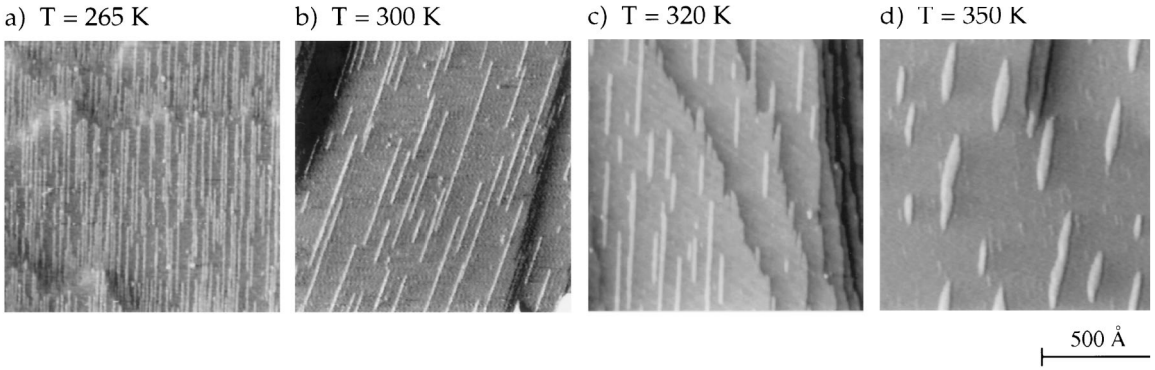

Figure 4: Illustration of two parameters to influence the morphology of self-assembled nanostructures: Cu/Pd(110). The uniaxial symmetry of the surface yields wires or elongated islands, while temperature influences both the density and size of the nanostructures (after [20]).

3 Self-organized epitaxial growth

Generally SO cannot arise from the growth mechanism solely, because inter-islands interactions are weak compared to island-substrate interactions, so that the initial random nucleation stage is kept during growth. Instead, SO can occur thanks to a self-organized pattern pre-existing on the substrate before deposition. SO will be competitive and of interest when the formation of structures intermediate between atomic size and the lithography resolution limit is achievable, *i.e.* around 10 nm. The interest in SO structures is not necessarily the order itself, but the improved monodispersion of structures' size as compared to SA, for example to reduce SNR in magnetic recording media, control the wavelength of quantum dot lasers, etc. Different types of SO strategies to fulfill this criterium are listed below.

3.1 Arrays of atomic steps

A vicinal surface of a single-crystal is a free surface whose orientation is slightly disoriented with respect to that of a low-Miller-index surface. Then, one or two Miller indices are small, the other(s) are large, for example (1 1 13), (1 17 0), (1 17 13), etc. Vicinal surfaces are usually fabricated by polishing a single crystal slightly off a low-Miller indices direction, with a disorientation called the *miscut angle*. When suitably prepared, at the atomic scale a vicinal surface consists of a regular array of parallel *atomic steps* separating atomically flat *atomic terraces* (Figure 5a), or an array of parallel accumulations of atomic steps separated by flat atomic terraces, a phenomenon called *step bunching* [5]. Step bunching can be viewed as a periodic micro-facetting of a surface. A 'suitable preparation' usually consists of an annealing, or a series ion etching/annealing to clean the surface, or (homo)epitaxial overgrowth, or a combination of several of these procedures. The occurrence of step bunching depends mainly on thermodynamic criteria like short-range step-step attractive forces. The length of bunched and flat areas depends on preparation conditions, *i.e.* on kinetic parameters.

Vicinal surfaces can be used as a template for further deposition ; this SO process is called *step decoration*. The idea is that the nucleation of adatoms along atomic steps is favored due to a higher coordination number. The growth temperature must be chosen high enough so that the mobility of adatoms if sufficient to reach atomic steps before nucleating clusters on terraces[4]. It is also advisable to choose a temperature not too high, so that alloying or intermixing can be avoided, and lower than the *two-dimensional evaporation temperature*[5], otherwise growth instabilities may develop [21]. Step decoration can result in the fabrication of dots clustered along steps [22], stripes (thin and large) [23, 24] or wires (thin and narrow down to the size of one atom) [25, 26] (Figure 5b).

3.2 Surface reconstructions

At a free surface the coordination number of atoms is smaller than in the bulk. A surface is said to be *reconstructed* when the lateral positions of the surface atoms differ–spontaneously– from a bulk atomic

[4]In other words, the distance between steps must be smaller than the mean distance $\ell(T)$ between islands that would be nucleated on an infinite flat terrace.

[5]Two-dimensional evaporation means that the adatoms stay on the surface, but can leave steps to wander again on terraces

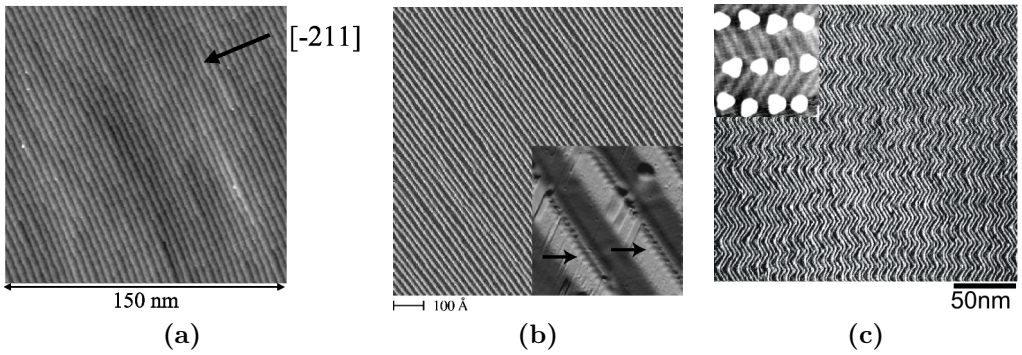

Figure 5: (a) Au(788), a vicinal surface, which is disoriented by 3.5 ° towards the [-211] azimuthal direction, with respect to Au(111) [27] (b) a mono-atomic Co wire self-organized on Pt(997) by step decoration [25] (c) Au(111) surface displaying the so-called *herringbone reconstruction*, with a period around 10 nm. Inset: 30 nm image displaying Co dots that self-organize on this surface [18].

plane of identical Miller indices[6], resulting in a multi-fold increase of the surface primitive cell. For semiconductors broken bonds often lead to the grouping of surface atoms, for example pairing to form rows, or more complex structures like for Si(7 × 7). For metals the density of states is increased at the surface, which favors smaller in-plane inter-atomic distances. In some instances, this results in the topmost plane being denser than in the bulk, inducing a long-range wavy structure to accomodate this plane with bulk ones, like in Au(001) or Au(111). The reconstruction of Au(111) is complex but useful for SO, for it has a cell size well above atomic distances, around 10 nm [28, 29]. A surface reconstruction often implies breaking of surface-symmetry.

Surface reconstructions can be used as a template for growth [1]. The adatoms can be trapped in a reconstruction cell, like for Si(111) [30], or nucleate via an atomic site-exchange process like for Ni, Co and Fe on Au(111) [31]. Note that the transfert of SO from the template to the overgrowth is not granted, and can be achieved only for selected systems and suitable growth conditions (Figure 5c).

3.3 Reconstructions due to adsorbates

Surface reconstructions can also be induced by the adsorbtion of sub-atomic-layer amounts of gases. Such reconstructions are more versatile than *intrinsic* reconstructions–*i.e.* without adsorbates– because they may exist whereas intrinsic reconstructions do not occur, or may be tailored changing the type of adsorbate or the adsorbed ratio. Besides, by adsorbing an amount of gas atoms smaller than that required to form a continuous reconstruction, patches of reconstructed areas are formed, in the same way as self-assembly naturally occurs in the sub-atomic-layer range. Then, owing to short-range attractive forces holding gaz atoms together, long-range repulsive forces elastically mediated through the substrate [32], and a relatively weak substrate/gas interactions, these patches may form a SO pattern, unlike deposits made of solid-state materials. The period is much larger than that of atoms, like for Cu:N or Cu:O with various orientations [33–35], and is therefore suitable for the overgrowth of nanostructures (Figure 5b).

The growth of metals, among which Au, Ni and Fe, have thus been used to fabricate arrays of dots or stripes on Cu(001) [36] and Cu(110), Fe stripes on Ir(001):H [37].

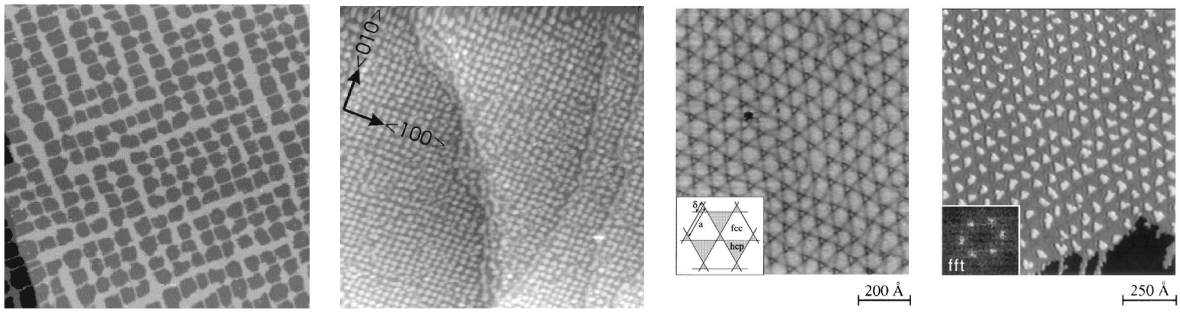

Figure 6: (a) 100 × 100 nm image of Cu(001):N (b) 200 × 200 nm image of 0.67 AL Au deposited on this surface [36] (c) Ag(2 AL)/Pt(111), deposited at 400 K, annealed at 800 K, and giving rise to an array of interface dislocations. Further deposition of a fraction of AL of Ag at 110K K yields an array of self-organized dots [3].

[6] A vertical displacement of the topmost atoms, *i.e.* a modification of the last inter-atomic distance, is always observed, usually a contraction. This effect is not called a reconstruction

3.4 Overlayer dislocations

For continuous hetero-epitaxial thin films a periodic lattice of dislocations may be found at the materials' interface. Such a lattice can be used as a template for SO. As a first step a hetero-epitaxial ultrathin film is deposited at temperature high enough to yield a flat surface, with a thickness just above the critical strain relaxation thickness to maximize the lateral modulation of chemical potential at the free surface, related to the array of buried dislocations. As a second step, the temperature is lowered so that newly-deposited adatoms remain trapped in the cells fenced by the dislocations, so that one dot is formed per cell. Example is Ag(sub-AL,110 K)/Ag(2 AL,400 K, annealing at 800 K)/Pt(111) (Figure 6c).

3.5 Wafer bonding and smart-cut

Arrays of buried dislocations can also be obtained without growth, by wafer bonding with a slight disorientation an ultra-thin mono-crystalline slab on a mono-crystalline substrate, making use of a smart-cut-like process ®. The geometry, the type of dislocations and the period of the interface dislocation network can be tailored by controlling the disorientation between the two single crystals. Then, if the top ultrathin layer is thinner than about the dislocation array period, a substantial adatoms chemical potential lateral modulation is induced at the surface resulting from the modulation of strainFigure 7a. This modulation can be used directly to achieve SO, or may be enhanced by a wet etching process prior to depositionFigure 7b. The ordering of subsequently grown materials is then increasedFigure 7c. These processes were proposed [41], first realized [38,39] and are still under active development [40,42] in CEA-LETI, Grenoble. The advantage of wafer bonding over misfit dislocations is that the period of the array can in principle be tuned continuously. The primary purpose is to provide a template for semiconductor quantum dots with a tunable size.

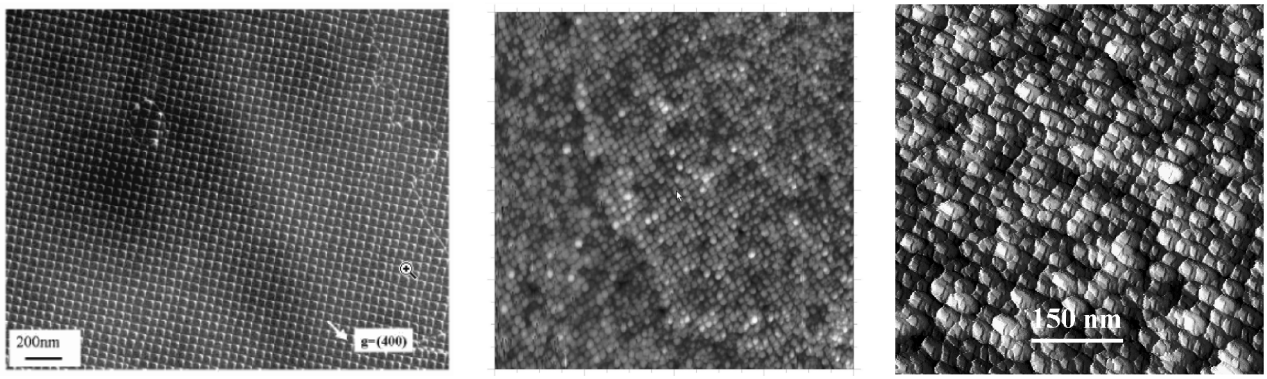

(a) **(b)** **(c)**

Figure 7: (a) top view high resolution electron microscopy of a bonded Si/Si sample, displaying a square array of screw dislocations [38,39]. The microscope reveals strains, while the surface remains almost flat (b) STM image of a similar sample, after subjection to a chemical etching, that revealed the array of stress into a topographical modulation [40] (c) Overgrowth of Ge on a chemically-revealed surface such as in (b) [40].

3.6 Interplay between steps and reconstructions

Two or more of the above-mentioned routes for SO can be combined, for instance vicinal surfaces and intrinsic reconstruction. This may result in an increase of the reconstruction cell size, along with a possible change of symmetry. In the case of Au(788) the reconstructions can be forced to run perpendicular to atomic steps, yielding a 2D array. This goes beyond 1D arrays from vicinal surfaces only, while removing the disadvantage that 120 °-rotated domains are found on Au(111) due to the three-fold symmetry of the surface. This process was used to produce a rectangular array of Co/Au(111) dots [27] and is under investigation for Fe/Au(788). Vicinal surfaces of Si were also used to stabilize triangular areas of (7×7) and (1×1) reconstructions with size up to hundreds of nanometers [43].

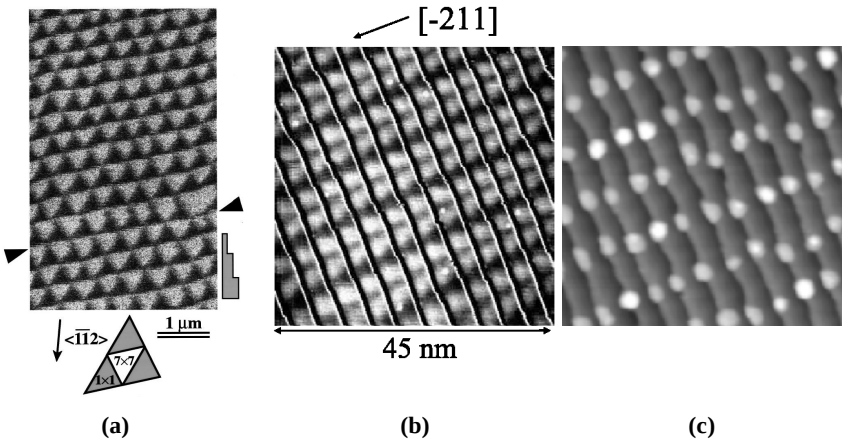

Figure 8: (a) Organization of (7×7) and (1×1) triangular domains on a slightly vicinal Si(111) surface [43] (b) On the Au(788) surface the reconstruction runs only perpendicular to the steps, inducing a tetragonal symmetry of the surface [27] (c) The surface shown in b can be used to grow a rectangular array of Co dots [27].

3.7 Self-organization from the deposit

As explained above, SO obtained directly during deposition is more rare because the interaction of a nanostructure with a substrate is of much higher magnitude than the interaction between neighboring nanostructures. However SO is sometimes observed in the case of the growth of alloys or mixtures of elements. In this case, a *lateral composition modulation* (LCM) might reduce epitaxial strain more effectively than a uniform film, analogously to the so-called *Grinfeld instability* [44] that favors the development of roughness in thick multilayers (Figure 9a). LCM is commonly observed in the growth of thick semiconductor alloys (Figure 9b). LCM has also been evidenced for ultrathin metal deposits consisting of two immiscible elements like CoAg or FeAg, leading to nanometers-wide chemical stripes (Figure 9c) [45]. In this latter case both immiscibility and strain relaxation are driving forces for the formation of the stripes (the compressive strain in Ag is balanced by the tensile strain in Co and Fe). Notice that LCM during growth is widely used in the fabrication of CoCr-based hard-disks media: during growth Cr segregates to grains boundaries between Co-rich grains, leading to the formation of columnar Co-rich magnetic structures. The average spacing between the columns is determined during the first stages of growth when nucleation takes place. A similar process was elegantly demonstrated to create a quasi-ordered array of ferromagnetic $CoFe_2O_4$ pillars in a piezoelectric $BaTiO_3$ matrix [46] (Figure 10a-b). This system displays

perpendicular magnetization with a fairly large anisotropy (Figure 10c), arising from a magneto-elastic contribution related to the strain in the pillars due to the surrounding matrix.

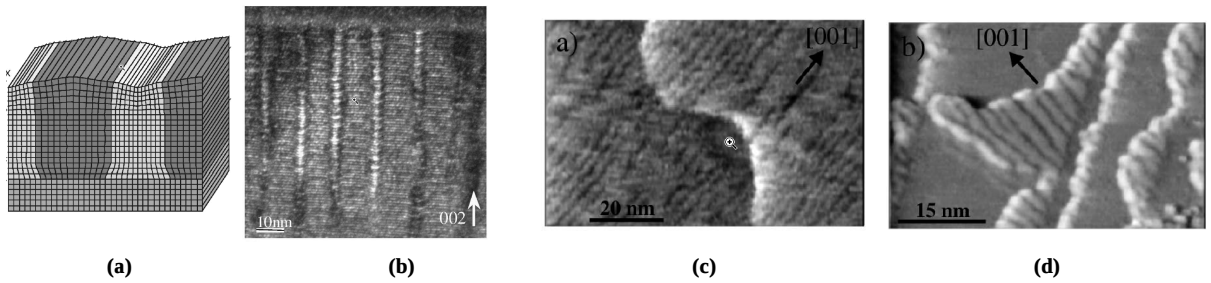

Figure 9: (a) Schematic illustration of the Grinfeld instability [47] (b) TEM micrograph of InAs/AlAs short-period multilayers [47]. Lateral Composition Modulation in the atomic layer range: FeAg(1 AL)/Mo(110) (c) and CoAg(0.3 AL)/Mo(110) [45].

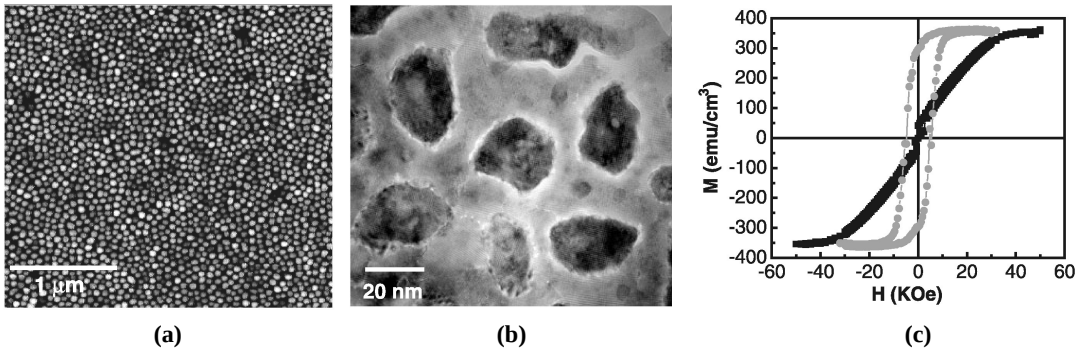

Figure 10: (a) AFM and (b) plane-view TEM images of an array of $CoFe_2O_4$ pillars in a piezoelectric $BaTiO_3$ matrix [46] (c) room-temperature hysteresis loops with the field applied perpendicular (shaded dots) and in-the-plane (black dots).

4 3D Self-organization via multilayers stacking

4.1 Examples and theory of vertical stacking

With a view to producing macroscopic amounts of quantum dots, multilayers of semiconductor SA dots have been fabricated. It has then been observed that dots from successive layers may have a tendency to pile up vertically [48] (Figure 11a), when the inter-layer spacing is thin enough[7]. This effect was explained by the strain induced by the hetero-epitaxial dots and mediated to the surface via the interlayer spacing [5]. This effect is therefore close to that used in Wafer-bonding (Sec.3.4,3.5).

[7] *Thin* must be understood when compared to the lateral size and/or nearest-neighbor distance between dots

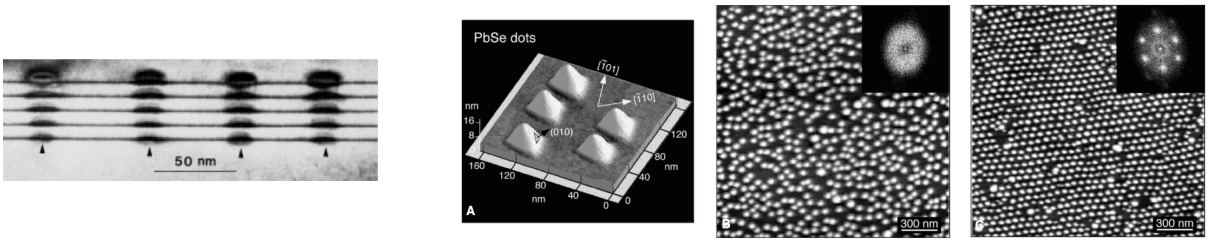

(a) **(b)** **(c)** **(d)**

Figure 11: (a) TEM micrograph of a multilayer of InAs/GaAs dots [48]. AFM views of PbSe/PbTe(111) dots: Close-up (b) and large-scale (c) views of the first layer of dots (d) large-scale view of the 60th layer of dots. Notice that in d the stacking of dots is of fcc type, which requires the (111) orientation and the highly anisotropic elastic behavior of the PbTe matrix [49].

4.2 From self-assembly to self-organization

A second effect is associated with the vertical stacking of dots. Whereas the dots of the first layer are SA, *i.e.* the in-plane order is of liquid-type with short-distance order (Figure 11a-b), after tens of multilayers the *lateral* order is observed to have greatly improved [49] (Figure 11d). This is again explained by theory rather simply with Marchenko's arguments [32] like in the case of partial adsorbate areas (partie 3.3) : lateral inter-dot interactions are repulsive due to strain, so that the lateral interdots spacings tend to become equal. This effect do not occur for a single deposit, as we explained above due to the strong interaction of the dot with the substrate, but can be progressively reached by tilting the 'columns' of dots through the stacking. A good organization can occur when the total height of the stacking becomes much larger than the lateral inter-dots spacing. These effect is similar to the Grinfeld instability mentioned afore [44], see partie 3.7 and Figure 9a.

4.3 Different types of stackings

Finally, different types of stackings symmetry could be obtained, depending on the orientation of the growth surface. Indeed, for highly elastically anisotropic materials, the effect of strain can be mediated in directions tilted with respect to the normal to the film, like in the case of PbTe(111) [49]. In this case it was shown by HREM and diffraction that a super-fcc array of dots could be formed. The topmost layer again displays an in-plane long-range order, with a hexagonal symmetry (Figure 11d).

5 Perspectives of self-organization

5.1 Towards self-organization engineering

In the previous sections we have listed the occurrences of SA and SO in categories and subcategories, in a pedagogical approach. However nature does not like boxes and drawers, and sometimes real situations cannot be disentangled into idealized cases. Besides, with a view to increasing the versatility of SO, it is a good idea to try to mix different approaches and change deposition conditions during the process. For example, we have mentioned the successful association of vicinal surfaces with reconstructions (partie 3.6), or the change of temperature during growth (partie 3.4). More can be done in the art of SO engineering, with the same spirit as in the case of continuous thin films were underlayers, separation layers and cappings can be suitably chosen. For example, a 3D SO super-stackings of dots can be performed with one set of materials with the purpose to create the lateral order, then switch to another material, required

for specific physical properties. It is also possible to change the deposition temperature and the spacer thickness to influence the size of dots or the area covered, respectively [50] (Figure 12). In the case of magnetism, such a process might be used to improve the monodispersion of grain size in recording media.

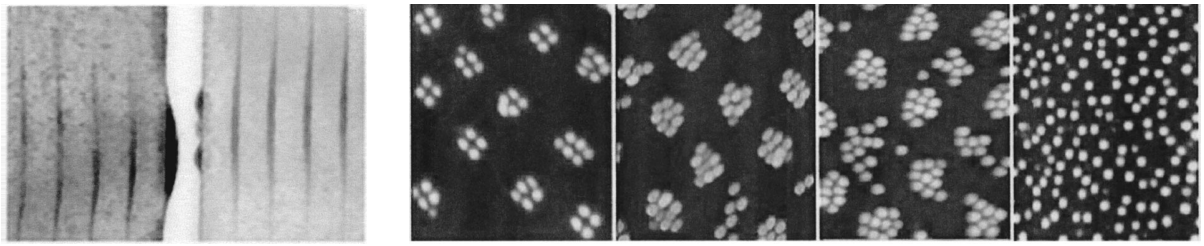

(a) **(b)**

Figure 12: (a) TEM micrographs of a Ge/Si(001) multilayer template grown at 750 °C (left) and the template used for overgrowth at 600 °C (right) (b) AFM images of the overgrowth at 600 °C as a function of Si spacer thickness (from left to right: 35 nm, 45 nm, 65 nm and 200 nm (after [50]).)

5.2 Self-organization on lithographic templates

Beside combining several epitaxial SO processes, one would also like to combine different techniques, like lithography and SO, the former to fabricate a pattern, the latter to growth defect-free nanostructures. This has already been achieved using annealed semiconductor MESAs, where the nucleation selectivity of more or less rough or stepped areas is used [51], or using oxide-based UHV compatible masks, *in situ* etching, followed by selective area epitaxy (SAE) [51–54] (Figure 13). Most examples come from the semiconductor community, because of the well-established cleaning procedures that allow surfaces to be prepared back to epitaxy-compatibility after lithographic procedures. Combination of lithography and SO remains a challenge for metals, although some results start to appear [55].

5.3 Self-organization beyond epitaxy

Finally, 3D SO super-stackings are not restricted to epitaxy. The stacking of Co clusters with layers of amorphous alumina were reported to give rise to a super-fcc stacking [56]. In this case, corrugation correlations are responsible for the progressive occurrence of order.

5.4 Structural characterization : scattering and super-diffraction

The development of new fields of physics often triggers the need for new characterization techniques. Apart from real imaging techniques, SO systems have been investigated by Xray scattering. When the order between nanostructures is sufficiently good, scattering resembles diffraction, with scattering vectors scaling inversely with the SO mesh size, not with atomic sizes. The, small-angle 'super-diffraction' [57] as well as satellite peaks around Bragg peaks [58] can be used. Information about size and spacing can be extracted, along with strain and chemical composition [1, 59].

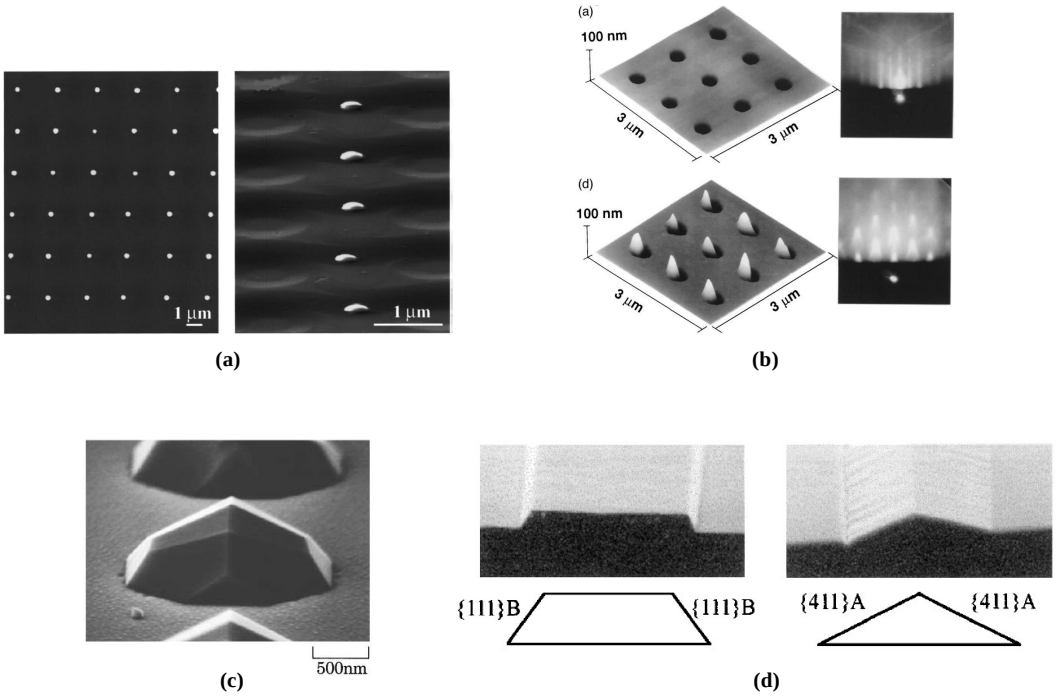

Figure 13: (a) Au droplets on Si(111) annealed mesas [53] (b) InAs/GaAs dots grown in holes fabricated *in situ* in an ultrathin oxide layer [52] (c) GaAs(001) homoepitaxy in holes through a SiO_2 mask [54] (d) same as c, but for stripes. The difference between left and right is the amount of GaAs redeposited [54].)

6 Self-organization for magnetic investigations

6.1 Potential applications of self-assembled dots

SO and SA cannot compete with lithography because the order and versatility are not sufficient for most industrial requirements. However they are competitive for producing large-area assemblies of dots in the low nanometer range, at or below the resolution of conventional replication lithography. Beyond the argument of low-cost, the advantage is to produce high-quality dots when one needs to develop physical properties that depend critically on the structure down to the atomic scale (in terms of microstructure and surface/interface quality). This is the case for semiconductors where defects can localize charge carriers, magnetism where interface defects induce irreproducible events, and catalysis that depends critically on the surface preparation.

The most promising prospects of potential applications concern SA deposits, where each dot is used independently, and the positional order plays no role. The deposit is taken as a whole, and considered as a material. This includes catalysis for metals deposited on oxides, and quantum dots for semiconductors. In the latter case there are serious prospects for high-efficiency laser, and more futuristic ideas of single-electron devices [1].

Concerning magnetism, mostly single-element metallic systems have been demonstrated, with however recent reports on oxydes [46, 60] and metallic alloys [61]. Concerning [46] the growth process ressembles that of columnar growth of conventional hard-disks media. Still, to date SO and SA are less advanced and

investigated for metals than for semiconductors, and no serious potential applications can be foreseen. However SO and SA systems can be used in research as model systems, to elucidate fundamental issues that cannot be disentangled from extrinsic effects in bigger or lithographic-produced nanostructures. Mainly, below are given examples of such studies.

6.2 Magnetic order in reduced dimension

SO has been used to mimic models of theoretical physics, like 2D or 1D spin networks. It has been confirmed that dipolar interactions, although weak, may help stabilize long-range magnetic order in low dimension. For example for Fe(0.8 AL)/W(110) stripes fabricated by step decoration the magnetization lies in-plane and perpendicular to the stripes, resulting in positive dipolar interactions. The microscopic picture of the ordering of this system is that exchange forces, that are strong but with a short range, induce the formation of spin blocks within each stripe, *i.e.* areas of single-domain magnetization; then positive dipolar forces that are weak but long-ranged prevent thermal fluctuation of these spin blocks within the 1D-stripes, thus ensuring the long-range ferromagnetic order [24] (Figure 14). Given the significant width of stripes, this system is intermediate between 2D and 1D. Concerning truly 1D systems, mono-atomic chains of Co were shown to remain non-ferromagnetic, although the magnetic correlation length may exceed the system's finite size in experiments [62]. Finally, when the system's dimensions become smaller than all characteristic magnetic length scales in all three directions, the magnetization is constraint to remain in a nearly single-domain state, usually called *macrospin*. Their remains only one effective degree of freedom, that is the orientation of the macrospin. The system can then be called 0D. It is stable at low temperature and becomes superparamagnetic above a critical temperature T_B, *i.e.* magnetization switching occurs spontaneously under thermal excitations (Figure 15).

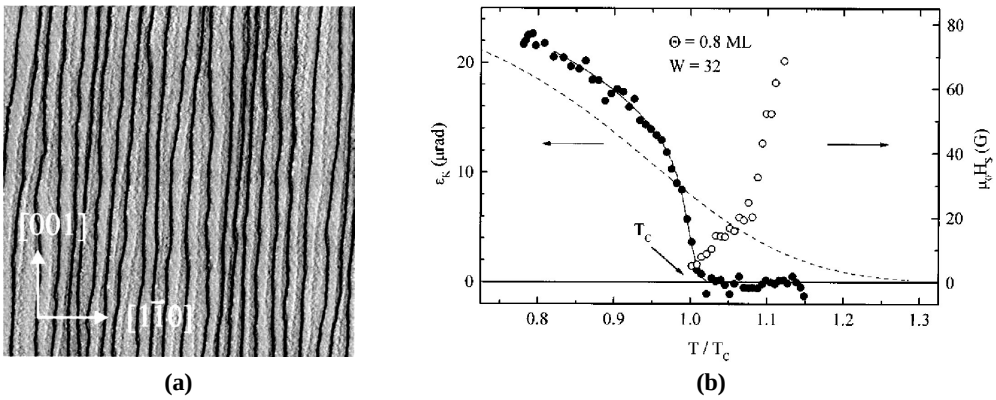

Figure 14: (a) 250×250 nm differentiated STM image of Fe/W(110) stripes self-organized by step decoration (b) Remanent magnetization (full dots) and low-field susceptibility (open dots) (Kerr ellipticity) as a function of temperature. The dotted line does not take into account the inter-stripes dipolar coupling, resulting in a broad distribution of Curie temperatures that does not fit experimental data. The full line is a fit that takes into account the coupling, with a good agreement with experiments (after [24]).

6.3 Anisotropy, from bulk towards atoms : steps, kinks and single atoms

Similarly to interfaces in continuous thin films, a symmetry breaking is expected at the edges and kinks of flat dots, the consequences of which are expected to dominate over bulk *and* top/bottom interfaces

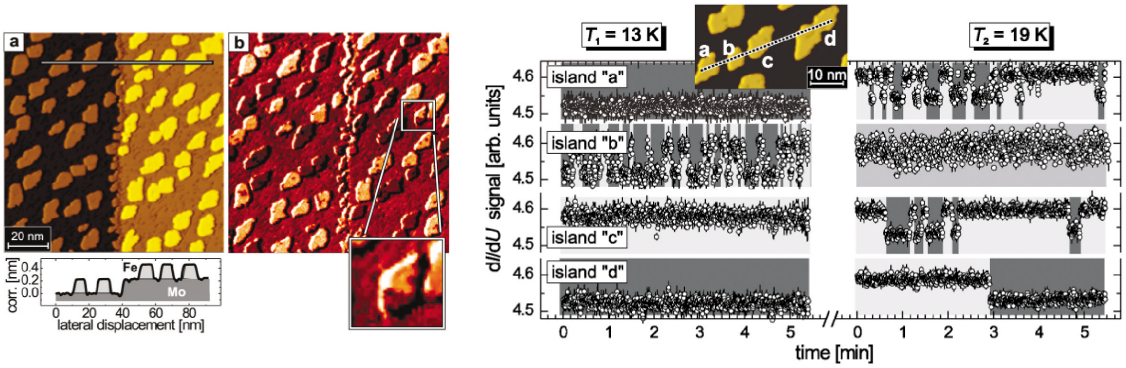

(a) **(b)**

Figure 15: (a) STM topographic (left) and magnetic (right) image of Fe(0.25 AL)/Mo(110) (b) Thermally-activated telegraphic switching of Fe dots macrospins as a function of temperature (after [63]).

Table 1: Orbital momentum and magnetic anisotropy energy (MAE) of Co/Pt(111) atoms as a function of coordination (after [62, 67]).

	bulk	mono-layer	bi-atomic wire	mono-atomic wire	two atoms	single atom
Orbital momentum (μ_B/at)	0.14	0.31	0.37	0.68	0.78	1.13
MAE (meV/at)	0.04	0.14	0.34	2.0	3.4	9.2

at small size. Owing to the deep sub-AL sensitivity of dichroism, it has become possible to investigate the evolution of spin and orbital moments of quasi-monodisperse assemblies of clusters [64, 65], stripes and wires down to monoatomic-width [62, 66], and eventually single atoms [67], and thus cover the entire range of properties from bulk to atoms. The orbital moment, essentially quenched in the bulk, rises progressively above 1 μ_B in single atoms. It was also revealed that, from the point of view of orbital moment and magnetic anisotropy energy, a cluster of two atoms (a bi-atomic wire, resp.) behaves closer to a wire (a mono-atomic slab, resp.) than to a single atom (a mono-atomic wire, resp.) (TAB. 1). This reminds us that the concept of dimensionality depends on the magnetic property studied: two atoms is closer to a wire when orbital momentum is concerned, but is close to a single atom when magnetic ordering is concerned. Quantum-confinement finite-size effects known in 2D were also shown to occur in 1D, like oscillatory anisotropy [68]. Finally, concerning spin moment, that of Co is essentially independent of size and shape, whereas that of Fe may vary considerably [65], which is explained by the sensitivity of Fe to structural changes, like in the bulk. Beyond SO systems, the newly-uncovered concept of enhanced edge anisotropy was applied to SA disks and tores of Co/Pt(111). It was shown that the total MAE of tores is similar to that of disks, because what counts is the edge atoms [19]. To confirm thin, MAE shrinks upon selective oxydation of the edges of such dots [69].

6.4 Model systems for micromagnetism

SO and SA are useful for fabricating and studying model micromagnetic systems, that cannot be achieved or are not suitable for investigation with a lithography process. Arguments in favor of SO are size below lithography resolution, quality of the system to access intrinsic properties, as well as its purity with respect

to the constraints associated with some investigation techniques, like spin-polarized STM. Quantitative analyses could thus be conducted on a series of issues. Geometrically constrained domain walls were observed with spin-polarized STM in SO Fe(1.5 AL)/W(110) stripes [70]: the width of domain walls shrinks at a constriction, because what counts is the total energy of the wall, *i.e.* energy per unit length times its length [71]. Surface magnetization states and magnetization processes were studied in atomically-flat dots of different size and shape, covering the range between 2D to near-bulk micromagnetism [72–74]. The surface size of magnetic vortices was measured, and was shown to expand (resp. shrink) when a perpendicular field is applied parallel (resp. antiparallel) to the magnetization direction of the core [75].

6.5 Thick self-organized systems: from surfaces to materials

Most self-organized magnetic systems were obtained in the range of sub-atomic-layer deposition. Thus, the resulting structures, either dots, stripes or wires, are very flat, generally one or two atomic layers high. Combined with their small lateral size, SO systems have a tiny volume. As a consequence they all are superparamagnetic at room temperature [19, 24, 62, 67, 76]: although atomic moments remain mostly parallel with each other at any time, the direction of the resulting moment, called a macrospin, fluctuates at the time scale of observation under the effect of thermal energy solely, because the magnetic anisotropy barrier that should prevent magnetization reversal roughly scales with the volume of the system, that is very small. Remanence and coercivity can be obtained at low temperature only. Such systems are therefore unsuitable for applications like storage. With a view to lifting this obstacle some growth processes were developed that allow one to grow SO systems with a height of several nanometers with no compromise on the order or the lateral density. This includes Co/Au(111) pillars [77] fabricated by sequential deposition of the two materials, Fe/cc(110) thick stripes cc=Mo,W fabricated by annealing a continuous film spontaneously grooved by buffer-layer-step-induced stress [78] (Figure 18), and ferromagnetic $CoFe_2O_4$ pillars in a piezoelectric $BaTiO_3$ matrix [46] (Figure 10) obtained by co-deposition. All these systems are magnetically at room temperature, *i.e.* they display significant remanence and coercivity.

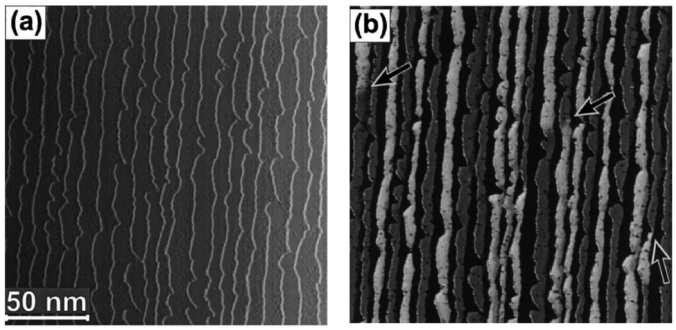

Figure 16: STM images of Fe(1.5 AL)/W(110) (a) differenciated topographic image (b) magnetic contrast (after [70]).

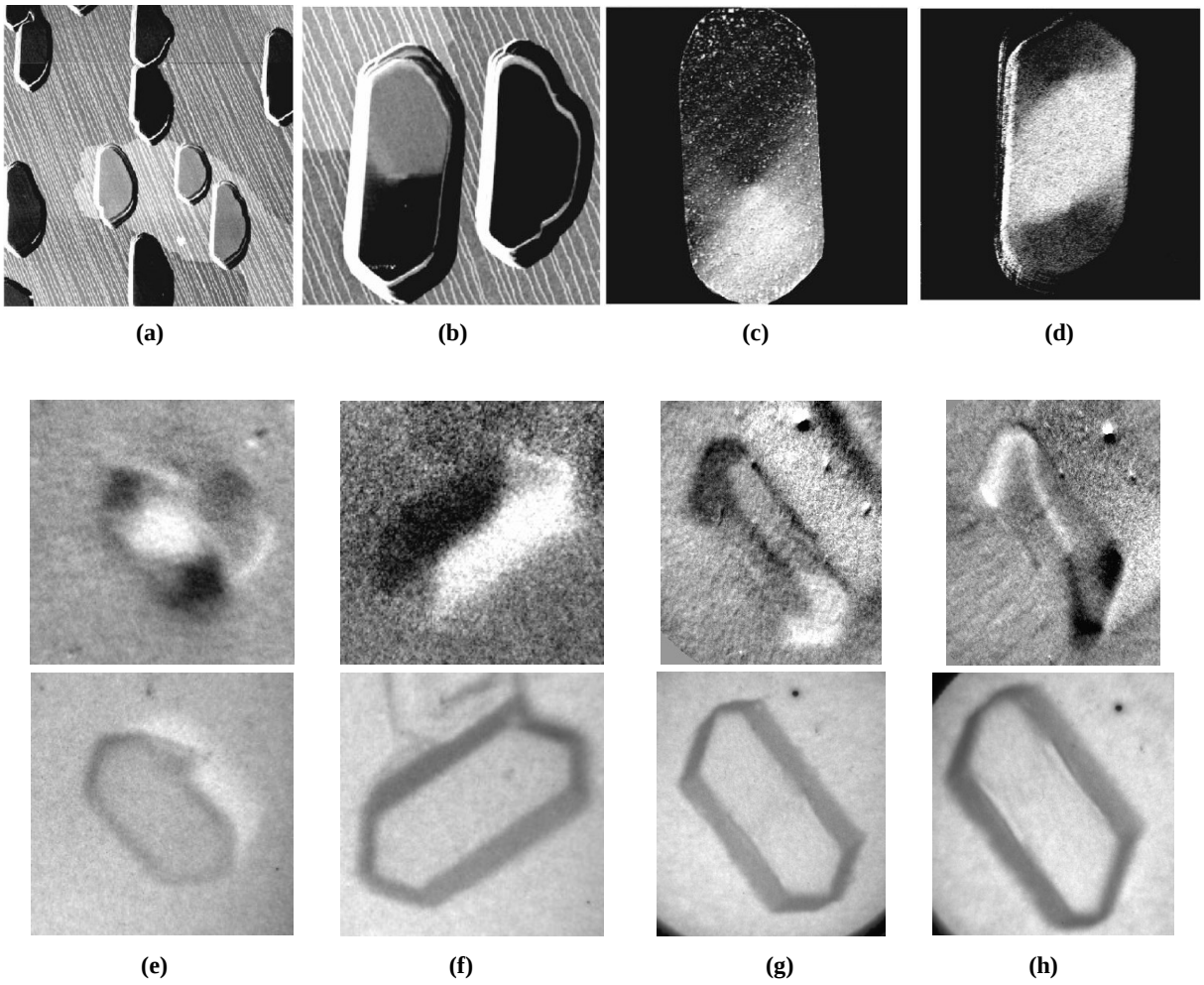

Figure 17: Surface magnetization state as a function of dot shape and size. (a-d) Fe/W(110) imaged with spin-polarized STM, with moderate vertical aspect ratio (height over width around 0.05) [72] and (e-h) Fe/Mo(110) imaged with X-PEEM, with a larger vertical aspect ratio, up to 0.25 [18]. Image size L and dot height h are given in nanometers following the notation $L; h$. (a) $1500; 3.5$, single-domain (b) $800; 4.5$, vortex-state (left) with $180\,^\circ$ walls (c) $500; 8$, vortex-state with $90\,^\circ$ walls (d) $700; 8.5$ diamond state (e) $1000; 65$ diamond state (f) $1000; 95$ symmetric Landau state (g) 1650(dot length); 180 asymmetric Landau state (h) 1600(dot length); 195 asymmetric Landau state with Néel-cap switch [18].

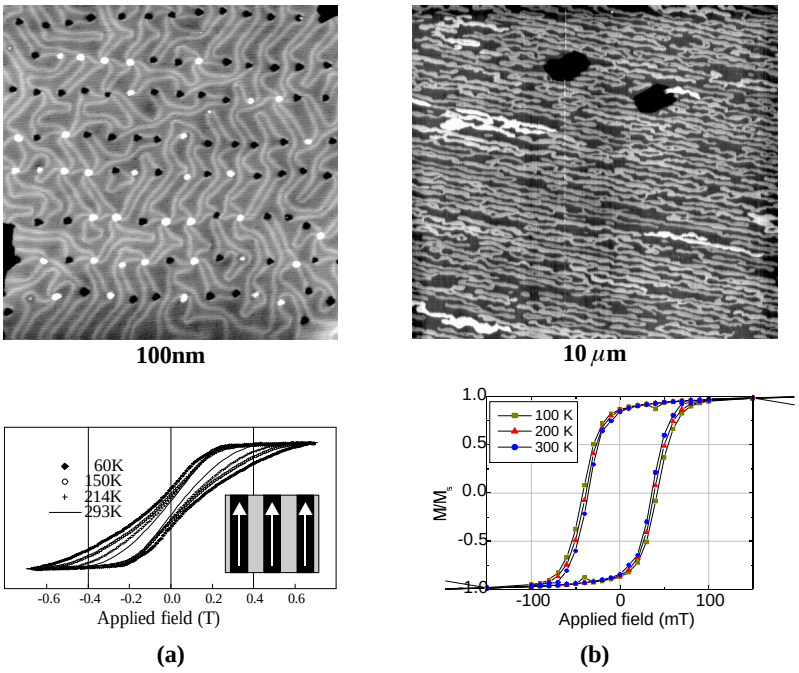

Figure 18: Two systems that are ferromagnetic and display remanence and coercivity at room temperature (bottom) (a) STM image taken during the course of fabrication of self-organized Co/Au(111) nanometers-high pillars, with perpendicular magnetization (b) AFM image of self-organized Fe/W(110) stripes 5.5 nm-high, with in-plane magnetization.

References

[1] `Special issue on Self-Organization, Ed. O. Fruchart. To appear in C. R. Phys. (Jan.2005), a journal of the French Academy of Sciences. Contributions from eight authors: growth, characterization, physical properties, both semiconductors and metals. See http://lab-neel.grenoble.cnrs.fr/pageperso/fruche/crphys/ for details.`

[2] H. Ibach, *The role of surface stress in reconstruction, epitaxial growth and stabilization of mesoscopic structures*, Surf. Sci. Rep. 29, 193–263 (1997), `review: surface stress measurement; surface stress for clean surfaces, with adsorbates, and deposits; mechanisms for self-organization.`

[3] H. Brune, *Microscopic view of epitaxial growth: nucleation and aggregation*, Surf. Sci. Rep. 31, 121–229 (1998), `review: diffusion of adatoms on surfaces and nucleation of islands; effect of symmetry, deposition and annealing temperature on islands' shape; self-organized surfaces and deposits.`

[4] A. Brune, Physical Properties of Thin Films and Artificial Multilayers, Vol. Sect. 1.9 of *Encyclopedia of Materials: Science and Technology*, Pergamon Press, 2001, Ch. Growth Modes, pp. 3683–3693, `review.`

[5] C. Teichert, *Self-organization of nanostructures in semiconductor heteroepitaxy*, Phys. Rep. 365, 335–432 (2002), `review: characterization techniques of self-organized surfaces; overview of phenomena giving rise to self-organization; 3D self-organization.`

[6] V. A. Shchukin, D. Bimberg, *Spontaneous ordering of nanostructures on crystal surfaces*, Rev. Mod. Phys. 71 (4), 1125–1171 (1999), `review: facetted surfaces; thermodynamics and kinetics of islands formation during growth; basics of 3D self-organization.`

[7] H. C. Jeong, E. D. Williams, *Steps on surfaces: experiments and theory*, Surf. Sci. Rep. 34, 171–294 (1999), `review: comprehensive review on steps, vicinal surfaces, etc.`

[8] J. I. Martin, J. Nogués, K. Liu, J. L. Vicent, I. K. Schuller, *Ordered magnetic nanostructures: fabrication and properties*, J. Magn. Magn. Mater. 256, 449–501 (2003), `review: broad overview of magnetic properties of nanostructures, with an emphasis on arrays (not necessarily self-organized). Very large number of relevant references; ideal as an entry point in the field.`

[9] L. Vitos, A. V. Ruban, H. L. Skiver, J. Kollár, *The surface energy of metals*, Surf. Sci. 411, 186–202 (1998), `an article reviewing the calculated and measured surface energy of nearly all elements, along several orientations.`

[10] E. Bauer, *Phänomenologische Theorie der Kristallabscheidung an Oberflächen*, I. Z. Kristallogr. 110, 372–394 (1958).

[11] F. C. Frank, J. H. van der Merwe, Proc. R. Soc. London Ser. A 198, 216 (1949).

[12] M. Volmer, A. Weber, *Keimbildung in übersättigten Gebilden*, Z. Physik. Chem. 119, 277–301 (1926).

[13] I. N. Stranski, L. Krastanov, *Zur Theorie der orientierten Ausscheidung von Ionenkristallen aufeinender*, Sitzungsbericht Akademie der Wissenschaften Wien, Math.-naturwiss. Kl. IIb 146 (1938).

[14] E. Bauer, Chemisorption systems, Vol. 3B of *The chemical physics of solid surfaces and heterogeneous catalysis*, Elsevier Science, Amsterdam, 1984, Ch. Metals on Metals, pp. 1–57.

[15] A. Zangwill, Physics at surfaces, Cambridge University Press, New-York, 1998.

[16] P.-O. Jubert, O. Fruchart, C. Meyer, *Self-assembled growth of facetted epitaxial Fe(110) islands on Mo(110)*, Phys. Rev. B 64, 115419 (2001).

[17] P. Müller, R. Kern, *Equilibrium nano-shape changes induced by epitaxial stress (generalised Wulf-Kaishew theorem)*, Surf. Sci. 457, 229–253 (2000).

[18] O. Fruchart *et al.*, `private data.`

[19] S. Rusponi, T. Cren, N. Weiss, M. Epple, L. Claude, P. Buluschek, H. Brune, *The remarkable difference between surface and step atoms in the magnetic anisotropy of 2D nanostructures*, Nature Mat. 2, 546 (2003).

[20] J. P. Bucher, E. Hahn, P. Fernandez, C. Massobrio, K. Kern, *Transition from one- to two-dimensional growth of Cu on Pd(110) promoted by cross-exchange migration*, Europhys. Lett. 27 (6), 473 (1994).

[21] V. Repain, G. Baudot, H. Ellmer, S. Rousset, *Two-dimensional long-range-ordered growth of uniform cobalt nanostructures on a Au(111) vicinal template*, Europhys. Lett. 58 (5), 730–736 (2002).

[22] K. Brunner, J. Zhu, C. Miesner, G. Abstreiter, O. Kienzle, F. Ernst, *Self-organized periodic arrays of SiGe wires and Ge islands on vicinal Si substrates*, Physica E 7 (3-4), 881–886 (2000).

[23] J. Shen, P. Ohresser, C. V. Mohan, M. Klaua, J. Barthel, J. Kirschner, *Low-spin and high-spin ferromagnetic fcc Fe ultrathin films on Cu(111) under slow and fast deposition*, in: 15th International Colloquium on Magnetic Films and Surfaces, Queensland, Australia, 1997, pp. 360–362.

[24] J. Hauschild, U. Gradmann, H. J. Elmers, *Perpendicular magnetization and dipolar antiferromagnetism in double layer nanostripe arrays of Fe(110) on W(110)*, Phys. Rev. B 57, R677 (1998).

[25] A. Dallmeyer, C. Carbone, W. Eberhardt, C. Pampuch, O. Rader, W. Gudat, P. Gambardella, K. Kern, *Electronic states and magnetism of monoatomic Co and Cu wires*, Phys. Rev. B 61 (8), R5133–R5136 (2000).

[26] S. Shiraki, H. Fujisawa, M. Nantoh, M. Kawai, *Confining Barriers for Surface State Electrons Tailored by Monatomic Fe Rows on Vicinal Au(111) Surfaces*, Phys. Rev. Lett. 92 (9), 096102–4 (2004).

[27] V. Repain, G. Baudot, H. Ellmer, S. Rousset, *Ordered growth of cobalt nanostructures on a Au(111) vicinal surface: nucleation mechanisms and temperature behavior*, Mater. Sci. Engineer. B 96, 178–187 (2002).

[28] A. R. Sandy, S. G. J. Mochrie, D. M. Zehner, K. G. Huang, D. Gibbs, *Structure and phases of the Au(111) surface: X-ray scattering measurements*, Phys. Rev. B 43 (6), 4667 (1991).

[29] J. V. Barth, H. Brune, G. Ertl, R. J. Behm, *Scanning tunneling microscopy observations on the reconstructed Au(111) surface: Atomic structure, long-range superstructure, rotational domains, and surface defects*, Phys. Rev. B 42 (15), 9307–9318 (1990).

[30] L. Vitali, M. G. Ramsey, F. P. Netzer, *Nanodot Formation on the Si(111)-(7 × 7) Surface by Adatom Trapping*, Phys. Rev. Lett. 83 (2), 316–319 (1999), `self-organization on a surface by adatom trapping in reconstruction cells`.

[31] J. A. Meyer, I. D. Baikie, E. Kopatzki, R. J. Behm, *Preferential island nucleation at the elbows of the Au(111) herringbone reconstruction through place exchange*, Surf. Sci. 365, L647–651 (1996).

[32] V. I. Marchenko, *On the elastic properties of crystal surfaces*, Sov. Phys. JETP 54, 605 (1981).

[33] K. Kern, H. Niehus, A. Schatz, P. Zeppenfeld, J. Goerge, G. Comsa, *Long-range spatial self-organization in the adsorbate-induced restructuring of surfaces: Cu{100}-(2 × 1)O*, Phys. Rev. Lett. 67, 855–858 (1991).

[34] F. M. Leibsle, S. S. Dhesi, S. D. Barrett, A. W. Robinson, *STM observations of Cu(100)-c(2 × 2)N surfaces: evidence for attractive interactions and an incommensurate c(2 × 2) structure*, Surf. Sci. 317 (3), 309–320 (1994).

[35] T. M. Parker, L. K. Wilson, N. G. Condon, F. M. Leibsle, *Epitaxy controlled by self-assembled nanometer-scale structure*, Phys. Rev. B 56 (11), 6458–6461 (1997).

[36] H. Ellmer, V. Repain, M. Sotto, S. Rousset, *Pre-structured metallic template for the growth of ordered, square-based nanodots*, Surf. Sci. 511, 183–189 (2002).

[37] A. Klein, A. Schmidt, L. Hammer, K. Heinz, *Lateral nanoscale Fe-Ir superlattices on Ir(100)*, Europhys. Lett. 65 (6), 830–836 (2004).

[38] K. Rousseau, J. L. Rouvière, F. Fournel, H. Moriceau, *Stability of interfacial dislocations in (001) silicon surfacial grain boundaries*, Appl. Phys. Lett. 80, 4121 (2002).

[39] F. Fournel, H. Moriceau, B. Aspar, K. Rousseau, J. Eymery, J.-L. Rouvière, N. Magnea, *Accurate control of the misorientation angles in direct wafer bonding*, Appl. Phys. Lett. 80 (5), 793–795 (2002).

[40] F. Leroy, J. Eymery, P. Gentile, F. Fournel, *Controlled surface nanopatterning with buried dislocation arrays*, Surf. Sci. 545 (3), 211–219 (2003).

[41] A. Bourret, *How to control the self-organization of nanoparticles by bonded thin layers*, Surf. Sci. 432, 37–53 (1999).

[42] J. Eymery, *Obtention d'un ordre à longue distance en surface grâce aux contraintes. Apport des collages moléculaires*, Habilitation à diriger des recherches, Université Joseph Fourier - Grenoble 1, Grenoble, `http://membres.lycos.fr/jeymery/` (2003).

[43] H. Hibino, Y. Homma, T. Ogino, *Triangular-tiled arrangement of* 7×7 *and* '1×1' *domains on Si(111)*, Phys. Rev. B 58 (12), R7500–7503 (1998).

[44] M. A. Grinfeld, Dok. Akad. Nauk SSSR 290, 1358 (1986).

[45] E. D. Tober, R. F. C. Farrow, R. F. Marks, G. Witte, K. Kalki, D. D. Chambliss, *Self-Assembled Lateral Multilayers from Thin Film Alloys of Immiscible Metals*, Phys. Rev. Lett. 81 (9).

[46] H. Zheng, J. Wang, S. E. Lofland, Z. Ma, L. Mohaddes-Ardabili, T. Zhao, L. Salamanca-Riba, S. R. Shinde, S. B. Ogale, F. Bai, D. Viehland, Y. Jia, D. G. Schlom, M. Wuttig, A. Roytburd, R. Ramesh, *Multiferroic* $BaTiO_3$-$CoFe_2O_4$ *nanostructures*, Science 303, 661–663 (2004).

[47] R. D. Twesten, D. M. Follstaedt, S. R. Lee, E. D. Jones, J. L. Reno, J. M. Millunchick, A. G. Norman, S. P. Ahrenkiel, A. Mascarenhas, *Characterizing composition modulations in InAs/AlAs short-period superlattices*, Phys. Rev. B 60 (19), 13619–13635 (1999).

[48] Q. Xie, A. Madhukar, P. Chen, N. Kobayashi, *Vertically self-organized InAs quantum box islands on GaAs(100)*, Phys. Rev. Lett. 75, 2542–2545 (1995).

[49] G. Springholz, V. Holy, M. Pinczolits, G. Bauer, *Self-Organized Growth of Three-Dimensional Quantum-Dot Crystals with fcc-Like Stacking and a Tunable Lattice Constant*, Science 282, 734 (1998).

[50] G. Capellinia, M. De Seta, C. Spinella, F. Evangelisti, *Ordering self-assembled islands without substrate patterning*, Appl. Phys. Lett. 82 (11), 1772 (2003).

[51] T. Ogino, H. Hibino, Y. Homma, *Step arrangement design and nanostructure self-organization on Si surfaces*, Appl. Surf. Sci. 117-118, 642–651 (1997).

[52] T. Ishikawa, S. Kohmoto, K. Asakawa, *Site control of self-organized InAs dots on GaAs substrates by in situ electron-beam lithography and molecular-beam epitaxy*, Appl. Phys. Lett. 73 (12), 1712–1714 (1998).

[53] Y. Homma, P. Finnie, T. Ogino, *Aligned island formation using an array of step bands and holes on Si(111)*, Appl. Phys. Lett. 74 (6), 815–817 (1999).

[54] H. Hasegawaa, H. Kuriyamaa, M. Itoa, Y. Horikoshia, *Area selective epitaxy of anti-dot structure of GaAs by solid source MBE*, J. Cryst. Growth 227-228, 1078–1083 (2001).

[55] R. Cheng, J. Pearson, H. F. Ding, V. Metlushko, S. D. Bader, F. Y. Fradin, D. Li1, *Self-assembled epitaxial magnetic lateral structures on Ru: Controlling the shape and placement*, Phys. Rev. B 69, 184409/1–5 (2004).

[56] D. Babonneau, F. Petroff, J.-L. Maurice, F. Fettar, A. Vaurès, A. Naudon, *Evidence for a self-organized growth in granular* Co/Al_2O_3 *multilayers*, Appl. Phys. Lett. 76 (20), 2892–2894 (2000).

[57] O. Fruchart, G. Renaud, A. Barbier, M. Noblet, O. Ulrich, J.-P. Deville, F. Scheurer, J. Mane-Mane, V. Repain, G. Baudot, S. Rousset, *X-ray super-cell crystallography of self-organized Co/Au(111) deposits*, Europhys. Lett. 63 (1), 135–141 (2003).

[58] B. Croset, Y. Girard, G. Prévot, M. Sotto, Y. Garreau, R. Pinchaux, M. Sauvage-Simkin, *Measuring Surface Stress Discontinuities in Self-Organized Systems with X Rays*, Phys. Rev. Lett. 88 (5), 056103/1–4 (2002).

[59] I. Kegel, T. H. Metzger, A. Lorke, J. Peisl, J. Stangl, G. Bauer, K. Nordlund, W. V. Schoenfeld, P. M. Petroff, *Determination of strain fields and composition of self-organized quantum dots using x-ray diffraction*, Phys. Rev. B 63, 035318 (2001).

[60] U. Lüders, F. Sánchez, J. Fontcuberta, *Initial stages in the growth of 111-faceted CoCr2O4 clusters: mechanisms and strained nanometric pyramids*, Appl. Phys. A 79 (1), 93–97 (2004).

[61] M. Albrecht, A. Maier, F. Treubel, M. Maret, R. Poinsot, G. Schatz, *Self-assembled magnetic nanostructures of* $CoPt_3$ *with favoured chemical ordering*, Europhys. Lett. 56 (6), 884–890 (2001).

[62] P. Gambardella, A. Dallmeyer, K. Maiti, M. C. Malagoli, W. Eberhardt, K. Kern, C. Carbone, *Ferromagnetism in one-dimensional monoatomic metal chains*, Nature 416, 301–304 (2002).

[63] M. Bode, O. Pietzsch, A. Kubetzka, R.Wiesendanger, *Shape-Dependent Thermal Switching Behavior of Superparamagnetic Nanoislands*, Phys. Rev. Lett. 92 (6), 067201/1–4 (2004).

[64] H. Dürr, S. Dhesi, E. Dudzik, D.Knabben, G. van der Laan, J. Goedkoop, F. Hillebrecht, *Spin and orbital magnetization in self-assembled Co clusters on Au(111)*, Phys. Rev. B 59 (2), R701–R704 (1999).

[65] P. Ohresser, N. B. Brookes, S. Padovani, F. Scheurer, H. Bulou, *Magnetism of small Fe clusters on Au(111) studied by X-ray magnetic circular dichroism*, Phys. Rev. B 64, 104429 (2001).

[66] P. Gambardella, *Magnetism in monatomic metal wires*, J. Phys.: Condens. Matter 15 (S2533-2546), `review`.

[67] P. Gambardella, S. Rusponi, M. Veronese, S. S. Dhesi, C. Grazioli, A. Dallmeyer, I. Cabria, R. Zeller, P. H. Dederichs, K. Kern, C. Carbone, H. Brune, *Giant magnetic anisotropy of single cobalt atoms and nanoparticles*, Science 300 (5622), 1130–1133 (2003).

[68] P. Gambardella, A. Dallmeyer, K. Maiti, M. C. Malagoli, S. Rusponi, P. Ohresser, W. Eberhardt, C. Carbone, K. Kern, *Oscillatory Magnetic Anisotropy in One-Dimensional AtomicWires*, Phys. Rev. Lett. 93 (7), 077203–1/4 (2004).

[69] T. Cren, S. Rusponi, N. Weiss, M. Epple, H. Brune, *Oxidation induced enhancement of magnetic susceptibility of Co islands on Pt(111)*, J. Phys. Chem. `In press`.

[70] M. Bode, O. Pietzsch, A. Kubetzka, R. Wiesendanger, *Imaging magnetic nanostructures by spin-polarized scanning tunnelling spectroscopy*, Journal of Electron Spectroscopy and Related Phenomena 114-116, 1055–1062 (2001).

[71] P. Bruno, *Geometrically Constrained Magnetic Wall*, Phys. Rev. Lett. 83 (12), 2425 (1999).

[72] M. Bode, A. Wachowiak, J. Wiebe, A. Kubetzka, M. Morgenstern, R. Wiesendanger, *Thickness dependent magnetization states of Fe islands on W(110): from single domain to vortex and diamond patterns*, Appl. Phys. Lett. 84 (6), 948–950 (2004).

[73] O. Fruchart, E. Bonet, J.-C. Toussaint, W. Wernsdorfer, *Nanomagnétisme : des domaines confinés au magnétisme moléculaire*, Bulletin de la S.F.P. 139, 11–17 (2003).

[74] O. Fruchart, J. C. Toussaint, P.-O. Jubert, W. Wernsdorfer, R. Hertel, J. Kirschner, D. Mailly, *Angular-dependence of magnetization switching for a multi-domain dot: experiment and simulation*, Phys. Rev. B 2004, `brief Report, in press`.

[75] A. Wachowiak, J. Wiebe, M. Bode, O. Pietzsch, M. Morgenstern, R. Wiesendanger, *Direct Observation of Internal Spin Structure of Magnetic Vortex Cores*, Sci. 298, 577–580 (2002).

[76] H. Takeshita, Y. Suzuki, H. Akinaga, W. Mizutani, K. Ando, T. Takayama, A. Itoh, K. Tanaka, *Magnetization process of a nanometer-scale cobalt dots array formed on a reconstructed Au(111) surface*, J. Magn. Magn. Mater. 165, 38–41 (1997).

[77] O. Fruchart, M. Klaua, J. Barthel, J. Kirschner, *Self-organized growth of nanosized vertical magnetic pillars on Au(111)*, Phys. Rev. Lett. 83 (14), 2769–2772 (1999).

[78] O. Fruchart, M. Eleoui, J. Vogel, P.-O. Jubert, A. Locatelli, A. Ballestrazzi, *Nanometers-thick self-organized Fe stripes: bridging the gap between surfaces and magnetic materials*, Appl. Phys. Lett. 84 (8), 1335–1337 (2004).

`[Date : 26th August 2004]`